Hindawi
International Journal of Antennas and Propagation
Volume 2019, Article ID 1564346, 9 pages
https://doi.org/10.1155/2019/1564346

Research Article

Novel Gysel Power Dividers with Negative Group Delay Characteristics

Zihui Zhu, Zhongbao Wang, Jianhao Zhou, Te Shao, Shaojun Fang, and Hongmei Liu

School of Information Science and Technology, Dalian Maritime University, Dalian, Liaoning 116026, China

Correspondence should be addressed to Zhongbao Wang; wzbdlmu@foxmail.com

Received 14 May 2019; Accepted 29 July 2019; Published 14 August 2019

Academic Editor: Giorgio Montisci

A novel Gysel power divider with negative group delay (NGD), good matching, and low insertion loss is proposed. Resistors connected with short-circuited coupled lines (RCSCL) are shunted at output ports of the Gysel power divider to obtain NGD characteristics, and another resistor is shunted at the input port to realize perfect input and output matching. To verify the proposed structure, an NGD Gysel power divider is designed and fabricated. At the center frequency of 1.0 GHz, the measured NGD times for different output ports are −1.94 ns and −1.97 ns, the input/output port return loss is greater than 38 dB, the insertion loss is less than 8.3 dB, and the isolation between output ports is higher than 41 dB. To enhance the NGD bandwidth, two RCSCL networks having slightly different center frequencies are connected in parallel, which provides wider bandwidth with good input matching characteristics.

1. Introduction

Power dividing is widely adopted for various microwave applications such as antenna feeding networks and amplifiers [1–4]. Because the branch-line hybrid coupler operating in simple power dividing needs an extra port, power dividers are used more commonly. Besides, the Gysel power divider has the advantages of high power-handling capability because of the external isolation resistors and monitoring capability for imbalances at the output ports [5]. Structure with negative group delay (NGD) characteristics has been used to enhance the efficiency of feed-forward amplifiers [6]. Usually, the time mismatch between the envelope and the RF paths in supply-modulated power amplifiers will decrease linearity [7] and cause instability [8]. NGD power dividers can be used to compensate the group delay through different transmission paths in the supply-modulated power amplifier. Recently, some NGD power dividers have been presented in [9–12]. However, only one output port of these power dividers has the NGD characteristics and suffers from very high insertion loss (IL), which is more than 15 dB. Therefore, a Wilkinson divider based on the shunt resistor that connected with short-circuited coupled lines is used to decrease the IL and obtain the NGD characteristics for two output ports [13]. A T-type divider based on a coupling matrix approach is presented in [14]. However, its isolation between output ports is less than 16 dB.

In this paper, a novel Gysel power divider with high power-handling capacity, good matching, low IL, and NGD characteristics is proposed. Design formulas are derived and both the theoretical and experimental results are given and discussed.

2. Design Theory

The schematic of the proposed NGD Gysel power divider is shown in Figure 1. It is based on the conventional Gysel power divider, which is composed of two-section transmission lines (TLs) with the characteristic impedance of Z_{01} and the electrical length of θ, two-section TLs with different characteristic impedance of Z_{02} and same electrical length of θ, and a TL with the characteristic impedance of Z_{03} and the electrical length of 2θ. And its output ports are, respectively, shunted by a resistor R_1 connected with short-circuited coupled lines (RCSCL) to realize the NGD characteristics. What's more, all the resistors are grounded directly or

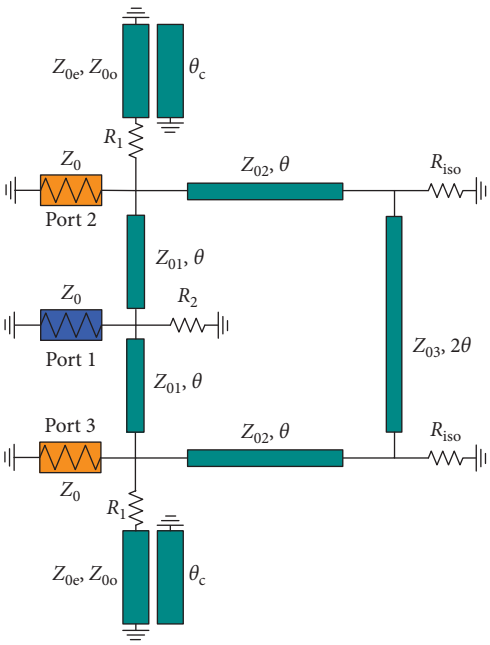

Figure 1: Configuration of the proposed NGD Gysel power divider.

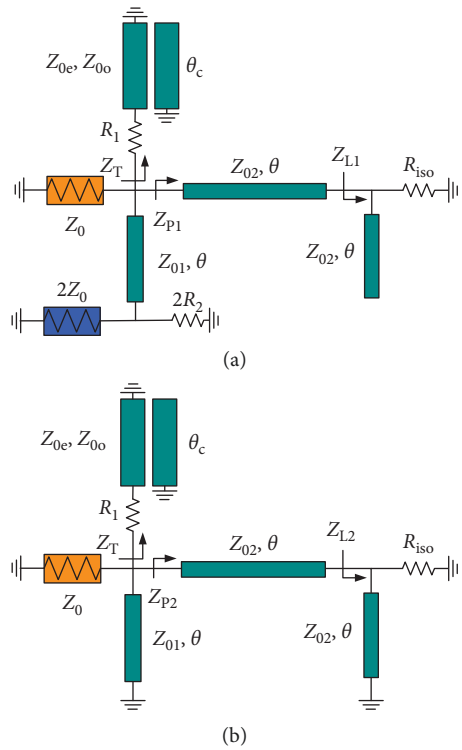

Figure 2: Equivalent circuits of the proposed NGD Gysel power divider. (a) Even-mode. (b) Odd-mode.

grounded by the coupled lines, which makes adequate heat sinking of the resistors possible; thus, the main power-limiting factor caused by the resistors will be decreased significantly, and it is better than the Wilkinson power divider with the power-handling capacity of 100-watt continuous wave [5]. The short-circuited coupled lines have an equivalent characteristic impedance of Z_c and electrical length of θ_c. Z_{0e} and Z_{0o} are the even- and odd-mode impedances of the coupled lines, respectively, which can be expressed as

$$Z_c = \frac{2Z_{0e}}{Z_{0e}/Z_{0o} - 1} = Z_{0e}\frac{1-k}{k} = Z_{0o}\frac{1+k}{k}, \tag{1}$$

where k is the coupling factor of the coupled lines. In addition, a resistor R_2 in parallel with the input port is added to realize perfect matching with port impedance Z_0. The even- and odd-mode equivalent circuits are shown in Figure 2.

The $ABCD$ matrix of the even-mode circuit are derived as

$$\begin{bmatrix} A & B \\ C & D \end{bmatrix} = \begin{bmatrix} 1 & 0 \\ \dfrac{1}{2R_2} & 1 \end{bmatrix} \begin{bmatrix} \cos\theta & jZ_{01}\sin\theta \\ \dfrac{j\sin\theta}{Z_{01}} & \cos\theta \end{bmatrix} \begin{bmatrix} 1 & 0 \\ \dfrac{1}{Z_T} + \dfrac{1}{Z_{P1}} & 1 \end{bmatrix}, \tag{2a}$$

with

$$Z_T = \frac{R_1 + jkZ_c\cot\theta_c}{\cot^2\theta_c - k^2\csc^2\theta_c}, \tag{2b}$$

$$Z_{P1} = \frac{Z_{02}\left(Z_{L1} + jZ_{02}\tan\theta\right)}{Z_{02} + jZ_{L1}\tan\theta}, \tag{2c}$$

$$Z_{L1} = \frac{R_{iso}\left(-jZ_{03}\cot\theta\right)}{R_{iso} - jZ_{03}\cot\theta}. \tag{2d}$$

The normalized $ABCD$ matrix elements are obtained as

$$a = \frac{A}{\sqrt{2}} = \frac{\left\{\cos\theta + jZ_{01}\sin\theta/Z_T + jZ_{01}\sin\theta/Z_{P1}\right\}}{\sqrt{2}}, \tag{3a}$$

$$b = \frac{B}{\sqrt{2}Z_0} = \frac{jZ_{01}\sin\theta}{\sqrt{2}Z_0}, \tag{3b}$$

$$c = \sqrt{2}Z_0C = \sqrt{2}Z_0 \cdot \left\{\frac{\cos\theta}{2R_2} + \frac{j\sin\theta}{Z_{01}} + \frac{\cos\theta}{Z_T} + \frac{\cos\theta}{Z_{P1}} + \frac{jZ_{01}\sin\theta}{2R_2Z_T} + \frac{jZ_{01}\sin\theta}{2R_2Z_{P1}}\right\}, \tag{3c}$$

$$d = \sqrt{2}D = j\sqrt{2}Z_{01}\frac{\sin\theta}{2R_2} + \sqrt{2}\cos\theta. \tag{3d}$$

The normalized S-parameters of even-mode can be expressed as

$$S_{11e} = \frac{a+b-c-d}{a+b+c+d}, \tag{4a}$$

$$S_{22e} = \frac{-a+b-c+d}{a+b+c+d}, \tag{4b}$$

$$S_{21e} = S_{12e} = \frac{2}{a+b+c+d}. \tag{4c}$$

Referring to Figure 2(b), the S-parameters of odd-mode can be expressed as

$$S_{22o} = \frac{Z_Q - Z_0}{Z_Q + Z_0}, \tag{5a}$$

with

$$Z_Q = \frac{(Z_T Z_{P2}/Z_T + Z_{P2}) jZ_{01} \tan\theta}{(Z_T Z_{P2}/Z_T + Z_{P2}) + jZ_{01}\tan\theta}, \tag{5b}$$

$$Z_{P2} = \frac{Z_{02}(Z_{L2} + jZ_{02}\tan\theta)}{Z_{02} + jZ_{L2}\tan\theta}, \tag{5c}$$

$$Z_{L2} = \frac{R_{iso}(jZ_{03}\tan\theta)}{R_{iso} + jZ_{03}\tan\theta}. \tag{5d}$$

Then, the S-parameters of the proposed NGD Gysel power divider can be calculated by using the even- and odd-mode scattering parameters as

$$S_{11} = S_{11e}, \tag{6a}$$

$$S_{21} = S_{31} = S_{13} = S_{12} = \frac{S_{21e}}{\sqrt{2}}, \tag{6b}$$

$$S_{22} = S_{33} = \frac{S_{22e} + S_{22o}}{2}, \tag{6c}$$

$$S_{23} = S_{32} = \frac{S_{22e} - S_{22o}}{2}. \tag{6d}$$

Applying the frequency-dependent electrical length of $\theta = \theta_c = \pi f/(2f_0)$, the group delay (GD) τ of the proposed NGD Gysel power divider can be obtained as

$$\tau = \tau_{21} = \tau_{31} = -\frac{d\angle S_{21}(f)}{d\omega} = -\frac{d\angle S_{31}(f)}{d\omega}. \tag{7}$$

For perfect matching of all the input/output ports and infinite isolation between two output ports at f_0, the following relations are found as

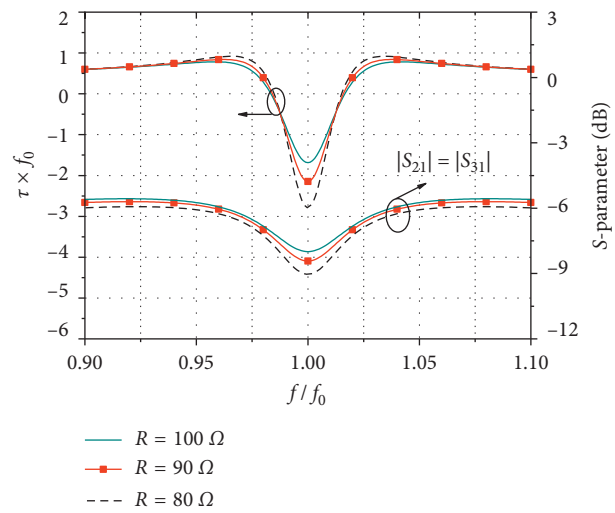

Figure 3: Effect of R on the IL and $\tau \times f_0$ of the proposed NGD power divider.

$$R_2 = R_1, \tag{8}$$

$$Z_{01} = Z_0\sqrt{\frac{2R_1R_2}{R_1R_2 - Z_0^2}}, \tag{9}$$

$$R_{iso} = \frac{(R_1 - Z_0)Z_{02}^2}{Z_0R_1}. \tag{10}$$

Moreover, the magnitude of transmission coefficient and group delay of the proposed NGD Gysel power divider at f_0 are, respectively, found as (11) and (12) assuming $R_1 = R_2 = R$.

$$|S_{21}(f_0)| = |S_{31}(f_0)| = \frac{2Z_0Z_{01}R^2}{\{Z_{01}^2(Z_0R + R^2 + Z_0^2 + Z_0R) + 2Z_0^2R^2\}}. \tag{11}$$

It can be found from (8), (9), and (11), the magnitude of transmission coefficient (i.e. IL) is only controlled by R. And (9) and (12) imply that R, k, Z_c, Z_{02}, and Z_{03} have effects on GD.

$$\tau_{21}\big|_{f=f_0} = \tau_{31}\big|_{f=f_0} = -\frac{\{-3Z_0Z_{01}Z_{02}^2R^3k + Z_0Z_{01}^2Z_{02}^2RZ_c - Z_0Z_{01}^2(Z_{02}+Z_{03})R^3k - Z_0^2Z_{01}Z_{02}^2R^2k + Z_0^2Z_{01}^2Z_{02}^2Z_c - 2Z_0^2Z_{01}Z_{02}^2R^2k - Z_0^2Z_{01}^2(Z_{02}+Z_{03})R^2k\}}{4f_0Z_{02}^2k(Z_0Z_{01}^2R^2 + Z_{01}^2R^3 + 2Z_0^2R^3 + Z_0^2Z_{01}^2R + Z_0Z_{01}^2R^2)}. \tag{12}$$

Figure 3 gives the effects of R on IL and $\tau \times f_0$ of the proposed NGD Gysel power divider with $Z_{02} = 100\,\Omega$, $Z_{03} = 100\,\Omega$, $k = 0.17$, and $Z_c = 550\,\Omega$. It can be observed that the maximum absolute value of NGD time at f_0 increases as R decreases from 100 to 80 Ω, but IL also increases. Therefore, there is a tradeoff between the IL and NGD time.

Figure 4 shows the calculated $\tau \times f_0$ of the proposed NGD Gysel power divider with $Z_{02} = 100\,\Omega$, $Z_{03} = 100\,\Omega$, and $R = 91\,\Omega$. As shown in Figure 4(a) for fixed $Z_c = 550\,\Omega$, the absolute value of NGD time at f_0 increases as k decreases from 0.19 to 0.15. However, the NGD bandwidth (i.e., the bandwidth for GD less than 0 ns) will be decreased. Similarly, increased Z_c leads to a larger absolute value of NGD

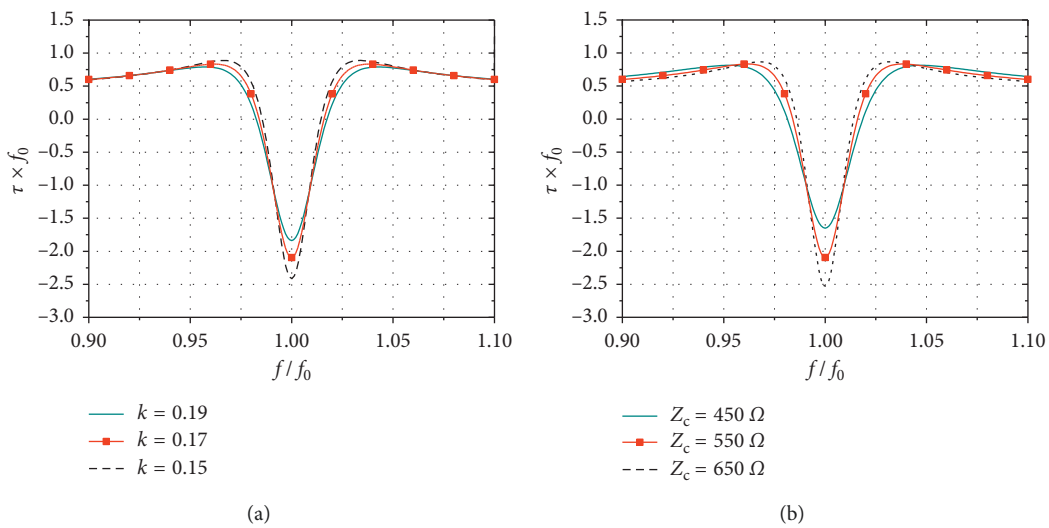

Figure 4: Effect of coupled lines on $\tau \times f_0$ of the proposed NGD power divider: (a) k. (b) Z_c.

time but narrower NGD bandwidth, which can be seen from Figure 4(b). Therefore, there is a tradeoff between the maximum absolute value of NGD time and the NGD bandwidth.

As shown in Figure 5(a), the absolute value of NGD time and NGD bandwidth will be improved when Z_{02} is increased. But there is a slight enhancement of the NGD time and bandwidth when Z_{02} is more than 100 Ω. Figure 5(b) shows that Z_{03} influences NGD characteristics slightly.

3. Circuit Layout and Implementation

3.1. Power Divider with Single-Stage RCSCL Networks. To verify the design concept of the proposed structure, an NGD Gysel power divider with single-stage RCSCL is designed with the center frequency of $f_0 = 1$ GHz, predefined NGD time of −2 ns, and IL less than 9 dB. The circuit is implemented on PTFE/woven-glass substrate with a relative permittivity of 2.65 and thickness of 1.5 mm.

In the design, R is first selected as 91 Ω for IL less than 9 dB. Using (9) with $R_1 = R_2 = R$, Z_{01} is calculated as 84.63 Ω to realize perfect input/output port matching at f_0. Referring to Figure 5, Z_{02} is selected as 100 Ω for obtaining a larger absolute value of NGD time, and Z_{03} is also selected as 100 Ω for simplicity. Then, R_{iso} is calculated as 90.1 Ω using (10). Based on Figure 4(b), after making a tradeoff between the NGD time and the NGD bandwidth, Z_c is selected as 530 Ω. Then, the coupling factor of the coupled lines is tuned with (12) to obtain the NGD time of −2 ns and determined as $k = 0.17$. Using (1), even- and odd-mode impedances of the coupled line are $Z_{0e} = 108.5$ Ω and $Z_{0o} = 77$ Ω, respectively. Furthermore, the electrical length of TLs at f_0 is $\theta_c = \theta = \pi/2$. Using the TL synthesis tool *ADS Linecalc*, the physical dimensions of TLs are calculated. However, optimal physical dimensions of TLs must take account of distributed capacitance effect of the strip open-ends and distributed inductance effect of via holes. Therefore, the final dimensions are obtained by using the HFSS EM simulation. At last, the

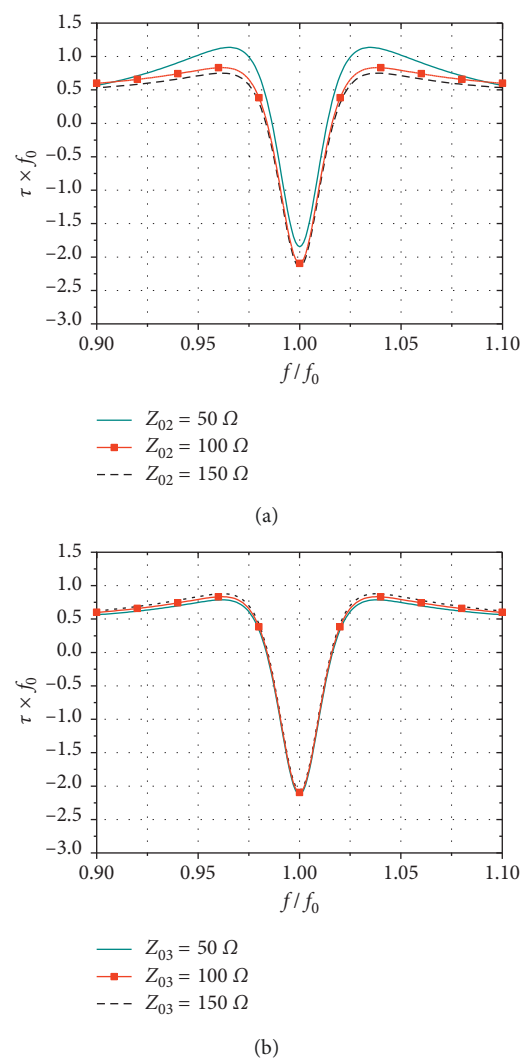

Figure 5: Effect of Z_{02} and Z_{03} on $\tau \times f_0$ of the proposed NGD Gysel power divider: (a) Z_{02}. (b) Z_{03}.

final dimensions of the NGD circuit are given in Table 1, and the photograph of the fabricated NGD Gysel power divider with $R_1 = R_2 = R_{iso} = 91\,\Omega$ is given as Figure 6. The overall circuit dimension is 82 mm × 79 mm.

The simulated and measured performances of the proposed NGD Gysel power divider are shown in Figure 7. The measured GD times at $f_0 = 1$ GHz for ports 2 and 3 are −1.94 ns and −1.97 ns, respectively. The measured NGD bandwidth of the proposed circuit is 31.3 MHz. The IL and IL bandwidth are shown in Figure 7(b), where IL bandwidth is defined as the 3 dB variation from the center frequency IL. The IL is 8.29 dB at f_0, and the measured IL bandwidth is 155 MHz. The return loss (RL) of input port 1 at f_0 is 44.4 dB and the RLs of output ports 2 and 3 are 38.3 dB and 40.1 dB, respectively. The measured isolation is 41.2 dB at f_0. Furthermore, the measured amplitude imbalance and phase differences between output ports 2 and 3 are ±0.05 dB and 0.55°, respectively.

The comparison of the proposed NGD Gysel power divider with other works is summarized in Table 2. The NGD power dividers [9–12] have larger NGD and IL bandwidths, but only one output port of the power divider has NGD characteristics and the IL is destructive (larger than 15 dB). Compared with [9–13], the proposed NGD Gysel power divider has a much lower IL. For the NGD power divider in [14], its isolation is poor (less than 16 dB), and it has a narrow IL bandwidth. The NGD power divider in [15] has the greatest IL bandwidth, but its output ports are not isolated (the isolation only is 1.2 dB). Except [12], the proposed NGD power divider has a better figure of merit (FOM). The FOM is defined as

$$\mathrm{FOM} = \frac{|\tau(f_0)| \times \mathrm{BW_{NGD}} \times \mathrm{BW_{IL}} \times |S_{21}(f_0)|}{f_0}. \tag{13}$$

This FOM definition takes $|\tau(f_0)| \times \mathrm{BW_{NGD}}$ to evaluate the performance of the NGD circuit. $|S_{21}|$ and $\mathrm{BW_{IL}}$ are added in the FOM for a better description of the transmission performance of the NGD circuit. At last, the relative bandwidth is introduced for a better comparison among different operation frequencies. Furthermore, the proposed power divider has the best RL performance with the smallest circuit size.

3.2. Power Divider with Parallel Connected Two-Stage RCSCL Networks. The NGD bandwidth of the power divider can be enhanced by using parallel connected NGD networks with slightly different center frequencies. However, the parallel connected RCSCL networks will change the port impedance of the ports 2 and 3. In order to match the 50-Ω port impedance, a simple method is to insert two $\lambda/4$ impedance transformers with the characteristic impedance of Z_{TF}, as shown in Figure 8.

For this purpose, the RCSCL networks are designed at $f_1 = 0.984$ GHz and $f_2 = 1.016$ GHz. For simplicity, most circuit element values of the Gysel power divider are same as previous, except for the values of resistances and the characteristic parameters of the coupled lines. R_a, R_b, Z_c, and k are selected as 41 Ω, 41 Ω, 350 Ω, and 0.28, respectively. To

Table 1: Dimensions of power divider with single-stage RCSCL networks (unit: mm; refer to Figure 6).

W_0	W_1	W_2	W_3	W_4	L_0	L_1	L_2
4.1	1.5	1.1	1.4	1.8	10	4.35	20.4
L_3	L_4	L_5	L_6	L_7	L_8	L_9	G_1
4.5	5.49	18.59	54	6.2	45	45.2	1.4

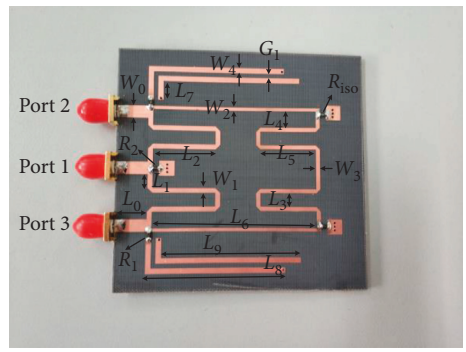

Figure 6: Photograph of the fabricated NGD Gysel power divider.

meet the requirement of zero reflection from three ports and infinite isolation between ports 2 and 3, R_c and R_d are determined as 59 Ω, and the characteristic impedance of the transformer is given as

$$Z_{TF} = \sqrt{\frac{Z_{02}^2 \times Z_0 \times Z_J}{Z_{02}^2 + Z_J \times R_d}}, \tag{14a}$$

with

$$Z_J = \left|\frac{Z_{T1} \times Z_{T2}}{Z_{T1} + Z_{T2}}\right|, \tag{14b}$$

$$Z_{T1} = R_a + \left.\frac{jkZ_c \cot(\theta_c f/f_1)}{\cot^2(\theta_c f/f_1) - k^2 \csc^2(\theta_c f/f_1)}\right|_{f=f_0}, \tag{14c}$$

$$Z_{T2} = R_b + \left.\frac{jkZ_c \cot(\theta_c f/f_2)}{\cot^2(\theta_c f/f_2) - k^2 \csc^2(\theta_c f/f_2)}\right|_{f=f_0}. \tag{14d}$$

The characteristic impedance of the impedance transformer is calculated as 36 Ω.

Taking the effect of parallel connection into consideration, the physical dimensions of the circuit are optimized using HFSS EM software. Finally, the dimensions of the NGD circuit with $R_a = 30\,\Omega$, $R_b = 47\,\Omega$, $R_c = 56\,\Omega$, and $R_d = 47\,\Omega$ are given in Table 3. The photograph of the fabricated power divider with parallel connected RCSCL networks is shown in Figure 9.

The simulated and measured performances of the NGD Gysel power divider with parallel connected RCSCL networks are shown in Figure 10. At f_0, the measured NGD and

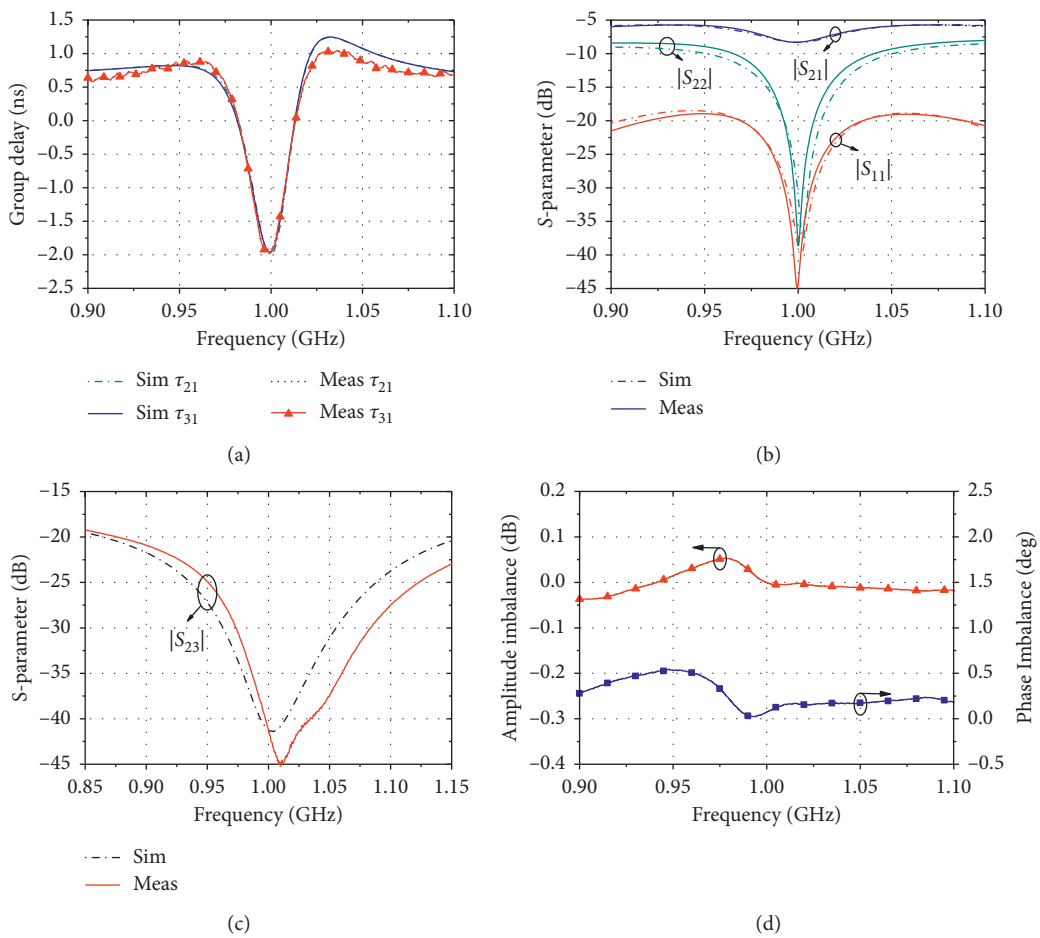

Figure 7: Performances of the proposed power divider. (a) Simulated and measured group delay. (b) Simulated and measured ILs and RLs. (c) Simulated and measured isolation. (d) Measured amplitude and phase imbalance characteristics.

Table 2: Performance comparison.

Ref.	f_0 (GHz)	NGD (ns)	NGD bandwidth (MHz)	IL (dB)	IL bandwidth (MHz)	RL (dB)	Isolation (dB)	FOM (10^{-3})	Size ($\lambda_g \times \lambda_g$)
[9]	1.00	−1.10*	250#	22.7	173	25.0	23.0	3.43	0.55 × 0.04
[10]	2.14	−0.53*	150	24.4	250	20.6	42.2	0.56	0.50 × 0.50
[11]	2.14	−0.48*	450	18.1	300	19.9	38.9	3.56	0.62 × 0.34
[12]	2.14	−0.48*	540+	15.0	410	37.0	34.9	8.88	0.61 × 0.76
[13]	2.14	−1.16	100	9.29	150	26.8	42.2	2.79	0.55 × 0.58
[14]	2.14	−0.56	55	6.97	100	17.5	15.8	0.62	0.94 × 0.48
[15]	2.14	−0.20	310	14.0	550	32.5	1.2	3.18	0.65 × 0.34
This work	1.00	−1.97	31.3	8.29	155	38.3	41.2	3.68	0.40 × 0.39

*Only one output port having NGD characteristics. #Results for two-section directional couplers. +Results for the example A in [12].

IL are obtained as −0.5 ns and 15.5 dB. In the mean time, the measured isolation is 33.3 dB, the RL of input port 1 is 40.3 dB, and the RLs of output ports 2 and 3 are 34.6 dB and 34.3 dB, respectively. The achievable GD time is obtained as −1.15 ± 0.65 ns with an NGD bandwidth of 62 MHz, which is wider than the power divider with single-stage RCSCL networks. Moreover, the 20-dB RL bandwidth of input port 1 is also wider. The maximum absolute value of NGD time is slightly less than the power divider with single-stage RCSCL networks, which is due to the positive GD of the impedance transformers. Furthermore, the measured amplitude imbalance between output ports 2 and 3 ranges from −0.2 to 0.1 dB and phase difference from −0.5 to 1.1 deg (Figure 10(d)).

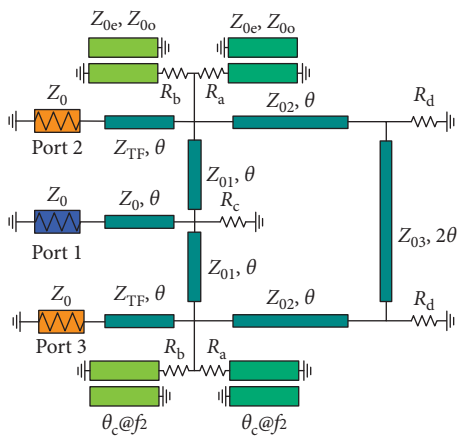

Figure 8: Configuration of the proposed power divider with parallel connected RCSCL networks.

Table 3: Dimensions of power divider with two-stage RCSCL networks (unit: mm; refer to Figure 9).

W_0	W_1	W_2	W_3	W_4	W_{TF}
4.1	1.1	1.1	1.1	1.42	7.8
L_0	L_1	L_2	L_3	L_4	L_5
51	7.8	18.9	4.5	5	23.9
L_6	L_7	L_8	L_9	G_1	
52.1	50.8	52.2	9.8	0.7	

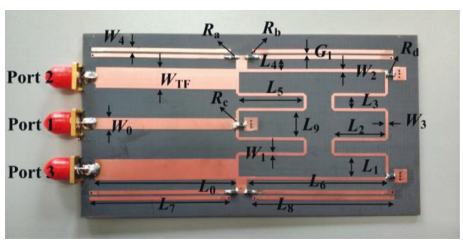

Figure 9: Photograph of the fabricated NGD Gysel power divider with parallel connected RCSCL networks.

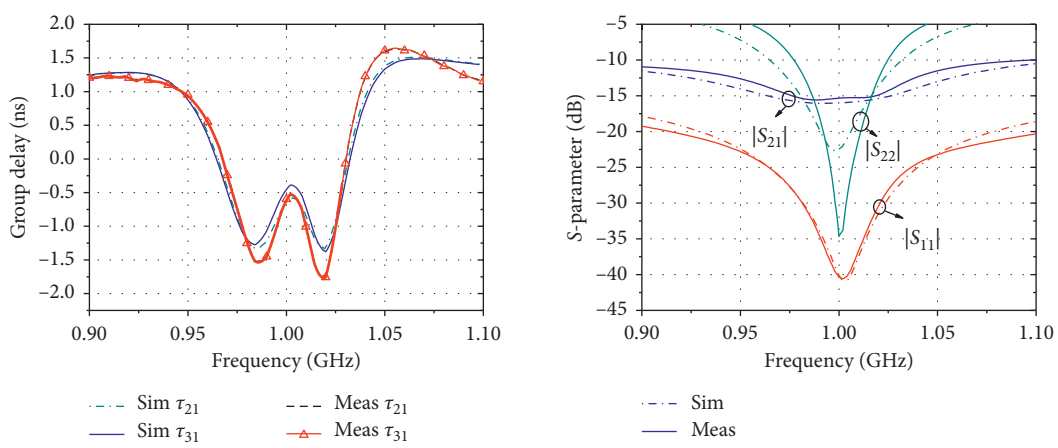

Figure 10: Continued.

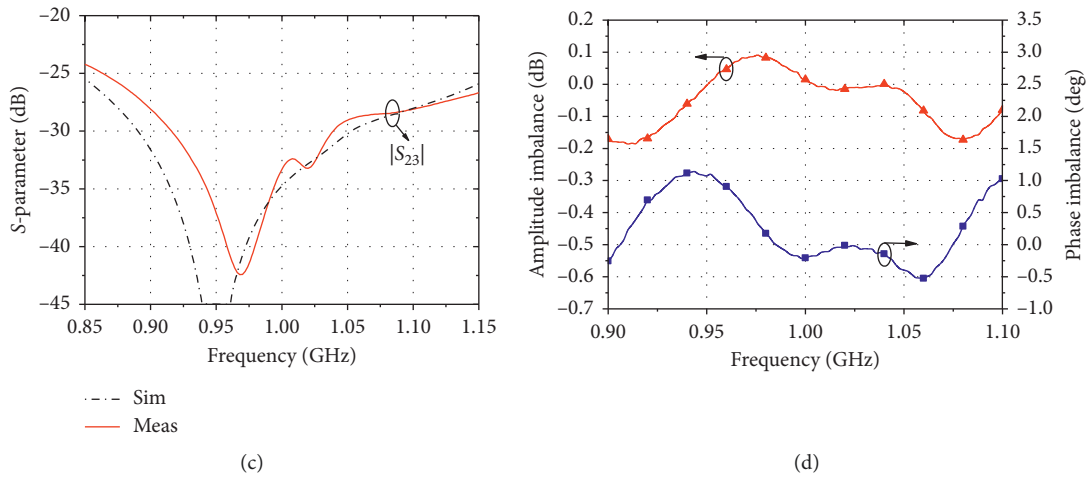

Figure 10: Performances of the Gysel power divider with parallel connected RCSCL networks. (a) Simulated and measured group delay. (b) Simulated and measured ILs and RLs. (c) Simulated and measured isolation. (d) Measured amplitude and phase imbalance characteristics.

4. Conclusions

In this paper, a novel Gysel power divider with NGD characteristics was proposed, which can be easily synthesized with the prescribed NGD time and IL. The analysis results show that a resistor shunted at the input port can be used to realize perfect matching, and the IL is controlled by the resistance value. What's more, a larger coupling factor k of the coupled lines results in a wider NGD bandwidth, and a larger equivalent characteristic impedance Z_c leads to a larger absolute value of NGD time. To enhance the NGD bandwidth, a Gysel power divider with parallel connected RCSCL networks was also presented in this paper. The proposed NGD power dividers have good RL, high isolation, and wide bandwidth, which can be applied to compensate group delay in microwave systems.

Data Availability

The data used to support the findings of this study are included within the article.

Conflicts of Interest

The authors declare that there are no conflicts of interest regarding the publication of this paper.

Acknowledgments

This work was supported in part by the National Natural Science Foundation of China under grant nos. 61871417, 61571075, and 51809030, in part by the Natural Science Foundation of Liaoning Province, in part by the Youth Science and Technology Star Project Support Program of Dalian City under grant 2016RQ038, and in part by the Fundamental Research Funds for the Central Universities under grant nos. 3132019219 and 3132019211.

References

[1] Q. Liu, Y. Liu, Y. Wu, M. Su, and J. Shen, "Compact wideband circularly polarized patch antenna for CNSS applications," *IEEE Antennas and Wireless Propagation Letters*, vol. 12, pp. 1280–1283, 2013.

[2] Q. Liu, Z. N. Chen, Y. Liu, F. Li, Y. Chen, and Z. Mo, "Circular polarization and mode reconfigurable wideband orbital angular momentum patch array antenna," *IEEE Transactions on Antennas and Propagation*, vol. 66, no. 4, pp. 1796–1804, 2018.

[3] Y. Wu, L. Jiao, Z. Zhuang, and Y. Liu, "The art of power dividing: a review for state-of-the-art planar power dividers," *China Communications*, vol. 14, no. 5, pp. 1–16, 2017.

[4] Y. Wu, Z. Zhuang, M. Kong, L. Jiao, Y. Liu, and A. A. Kishk, "Wideband filtering unbalanced-to-balanced independent impedance-transforming power divider with arbitrary power ratio," *IEEE Transactions on Microwave Theory and Techniques*, vol. 66, no. 10, pp. 4482–4496, 2018.

[5] U. H. Gysel, "A new N-way power divider/combiner suitable for high-power applications," in *Proceedings of the IEEE-MTT-S International Microwave Symposium*, pp. 116–118, IEEE, Palo Alton, CA, USA, May 1975.

[6] H. Choi, Y. Jeong, C. D. Kim, and J. S. Kenney, "Efficiency enhancement of feedforward amplifiers by employing a negative group-delay circuit," *IEEE Transactions on Microwave Theory and Techniques*, vol. 58, no. 5, pp. 1116–1125, 2010.

[7] K. Bumman, M. Junghwan, and K. Ildu, "Efficiently amplified," *IEEE Microwave Magazine*, vol. 11, no. 5, pp. 87–100, 2010.

[8] Z. Popovic, "GaN power amplifiers with supply modulation," in *Proceedings of the IEEE MTT-S International Microwave Symposium*, pp. 1–4, IEEE, Phoenix, AZ, USA, May 2015.

[9] C.-T. M. Wu and T. Itoh, "Maximally flat negative group-delay circuit: a microwave transversal filter approach," *IEEE Transactions on Microwave Theory and Techniques*, vol. 62, no. 6, pp. 1330–1342, 2014.

[10] G. Chaudhary, J. Park, Q. Wang, and Y. Jeong, "A design of unequal power divider with positive and negative group delays," in *Proceedings of the European Microwave Conference*, pp. 127–130, EUMC, Paris, France, September 2015.

[11] G. Chaudhary, P. Kim, J. Jeong, and Y. Jeong, "A power divider with positive and negative group delay characteristics," in *Proceedings of the URSI Asia-Pacific Radio Science Conference*, pp. 1195–1197, URSI, Seoul, Korea, August 2016.

[12] Y. Wu, H. Wang, Z. Zhuang, Y. Liu, Q. Xue, and A. A. Kishk, "A novel arbitrary terminated unequal coupler with bandwidth-enhanced positive and negative group delay characteristics," *IEEE Transactions on Microwave Theory and Techniques*, vol. 66, no. 5, pp. 2170–2184, 2018.

[13] G. Chaudhary and Y. Jeong, "A design of power divider with negative group delay characteristics," *IEEE Microwave and Wireless Components Letters*, vol. 25, no. 6, pp. 394–396, 2015.

[14] G. Chaudhary and Y. Jeong, "A finite unloaded quality-factor resonators based negative group delay circuit and its application to design power divider," *Microwave and Optical Technology Letters*, vol. 58, no. 12, pp. 2918–2921, 2015.

[15] H. Wang, Y. Wu, Z. Wu, W. Wang, and Y. Liu, "Compact arbitrary terminated power divider with bandwidth-enhanced negative group delay characteristics," *International Journal of Circuit Theory and Applications*, vol. 47, no. 6, pp. 909–916, 2019.